Journal of Marine Research, 72, 1–18, 2014

Thermohaline staircases in the western Mediterranean Sea

by Harry L. Bryden[1,2,3], Katrin Schroeder[4], Stefania Sparnocchia[5], Mireno Borghini[3] and Anna Vetrano[3]

ABSTRACT

Thermohaline staircase structures are commonly observed in the western Mediterranean Sea within the halocline-thermocline connecting the Levantine Intermediate Water at about 400 m depth with the western Mediterranean deep waters below 1,500 m. In this halocline-thermocline where warmer, saltier waters overlie colder, fresher deep waters, salt finger mixing processes are thought to be active and produce staircases with layers of order 75 m thickness containing nearly constant properties separated by sharp steps of order 6 m thickness with jumps in properties between the layers. While the layers have nearly constant salinity, potential temperature, and potential density, each property decreases very slightly downward through the layer so that it appears that salinity, heat, and density are being put into the top of each layer and then convectively mixing downward through the layer. Such observations are consistent with salt finger processes that transport salinity, heat and density downward through the halocline-thermocline.

Using repeat occupations of stations across the southern western Mediterranean Sea in 2006, 2008, and 2010, we have calculated downward salt transport, F_S, of 5.35×10^{-8} psu m s^{-1}, and downward heat transport, F_T, of 12.4×10^{-8} °C m s^{-1}. After multiplying these fluxes by haline contraction (β) and thermal expansion (α) coefficients respectively, the buoyancy flux ratio, $\alpha F_T/\beta F_S$, is found to be 0.74 and there is a downward density flux of 1.0×10^{-10} W kg^{-1}. The halocline-thermocline in this region between 600 and 1,400 dbar has a background vertical salinity gradient of 0.95×10^{-4} m^{-1} and a vertical temperature gradient of 4.1×10^{-4} °C m^{-1} so the background density ratio is $R_\rho = (\alpha d\theta/dz)/(\beta dS/dz)$ is 1.28. Dividing the downward fluxes by the background vertical gradients yields vertical diffusivities $k_S = 5.6 \times 10^{-4}$ m^2 s^{-1} and $k_T = 3.0 \times 10^{-4}$ m^2 s^{-1}. These downward fluxes of salt and heat are compared with estimates based on salt finger experiments and theory and with the long-term increases in salinity and temperature in the deep western Mediterranean Sea over the past 40 years.

1. Ocean and Earth Science, University of Southampton, Empress Dock, Southampton, SO14 3ZH, United Kingdom.

2. Corresponding author ***e-mail: h.bryden@noc.soton.ac.uk***

3. Istituto di Scienze Marine (ISMAR), Consiglio Nazionale delle Ricerche (CNR), Forte Santa Teresa, 19032 Lerici (SP), Italy.

4. Istituto di Scienze Marine (SMAR), Consiglio Nazionale delle Ricerche (CNR), Arsenale – Tesa 104, Castello 2737/F, 30122 Venice, Italy.

5. Istituto di Scienze Marine (ISMAR), Consiglio Nazionale delle Ricerche (CNR), Viale Romolo Gessi 2, 34123 Trieste, Italy.

1. Introduction

In the western Mediterranean, a core of Levantine Intermediate Water (LIW) at about 400 dbar enters from the eastern Mediterranean through the Sicily Channel, circulates northward to the west of Sicily and then counterclockwise around the basin and enters the Alboran Sea near the southeast coast of Spain (Katz, 1976). LIW is identified by a maximum salinity (and sometimes temperature) near 400 dbar throughout the western Mediterranean. Deep water is formed in the northwestern Mediterranean in the Gulf of Lion during severe winters. In a sense the LIW salinity maximum preconditions the water column for deep water formation so that during a severe winter heat loss cools the surface waters until they are dense enough to mix down through the high salinity LIW core. Continued heat loss (and associated evaporation) leads to the formation of deep water which then spreads throughout the western Mediterranean basin. The deep water is naturally colder and fresher than the high salinity, high temperature core of LIW. Thus, the vertical water mass structure below 200 m in the western Mediterranean exhibits a warm, salty core of LIW at about 400 m, a halocline-thermocline from about 400 m to 1600 m depth, and colder, fresher western Mediterranean deep waters below 1,600 m (Fig. 1).

The average vertical temperature, salinity, and density gradients in the main halocline-thermocline between 600 dbar and 1,400 dbar in the southern western Mediterranean Sea for stations 5 to 16 (Fig. 2) are 4.09×10^{-4} °C m^{-1}, 0.953×10^{-4} m^{-1} and 2.04×10^{-5} kg m^{-4}. Temperature stratification is stabilizing while the salinity stratification is destabilizing and the overall density gradient is small, with only a change in density of 16×10^{-3} kg m^{-3} over the 800 m depth range of the main halocline-thermocline. Based on these large-scale gradients, the density ratio, $R_\rho = (\alpha d\theta/dz)/(\beta dS/dz)$ is 1.28, where $\beta = 7.44 \times 10^{-4}$ psu^{-1}* and $\alpha = 2.20 \times 10^{-4}$ °C^{-1} are haline contraction and thermal expansion coefficients respectively. In such stratification with warmer, saltier waters above colder, fresher waters below, salt finger processes are expected to be active (Turner, 1973). Salt finger mixing is thought to be more active the closer R_ρ is to 1, which is the point where the salinity gradient is balanced by the temperature gradient and there is no density stratification. Evidence for salt finger mixing has traditionally been the observation of a series of layers and steps in the halocline-thermocline where warmer, saltier water overlies colder fresher waters. Indeed thermohaline staircase structures have regularly been observed in the Mediterranean Sea (Johannessen and Lee, 1974; Molcard and Tait, 1977; Zodiatis and Gasparini, 1996). Here we describe new observations of thermohaline staircase structures in the southern Western Mediterranean Sea during 2006, 2008, and 2010, we estimate the vertical salt and heat fluxes, and we compare the observed staircase properties with theoretical models.

*Salinity is formally a ratio and has no units. When vertically integrating or differentiating salinity, we find it useful to add the symbol psu to represent salinity in the integrated values or in the gradients so the units are clear and further calculations are understandable.

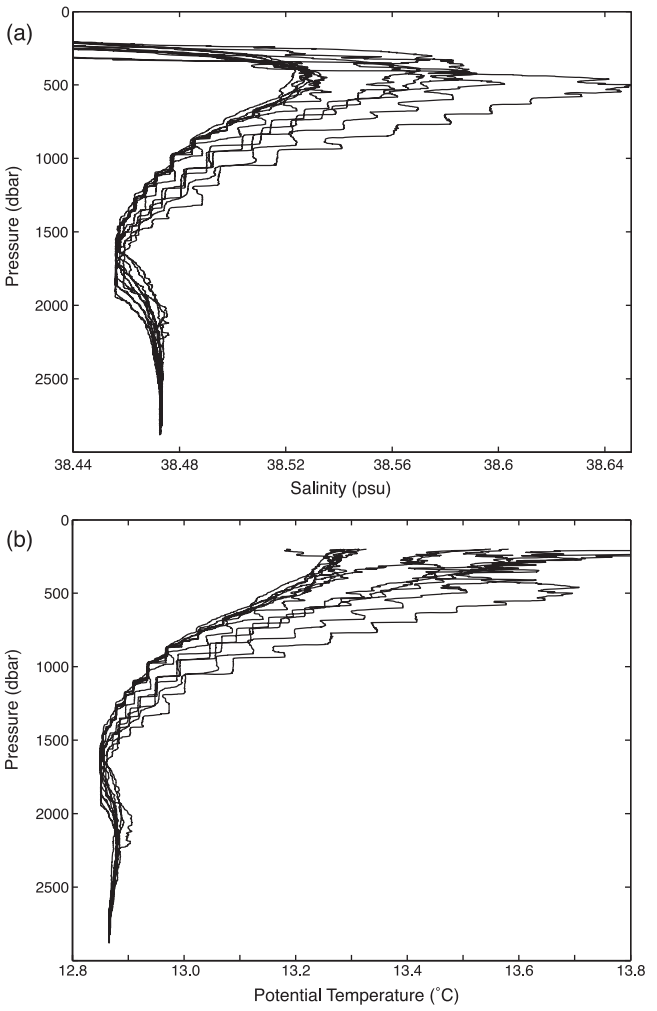

Figure 1. Profiles of (a) salinity and (b) potential temperature below 200 dbar at stations 5 to 16 for the 2008 survey. Note the maximum in salinity at about 400 dbar at each station associated with the core of Levantine Intermediate Water. Below the intermediate water maximum, there is a halocline-thermocline exhibiting thermohaline staircase structures that connects the warmer, saltier intermediate water with the colder, fresher deep western Mediterranean waters. We determine the background vertical potential temperature and salinity gradients from the average 600 to 1,400 dbar gradients for these stations.

2. Staircase structures in the halocline-thermocline

Stations 4 to 17 were taken in October 2006, November 2008, and August 2010 (Fig. 2). At each station a CTD/LADCP/Rosette package was lowered from the surface to the bottom. The SeaBird CTD profiles of temperature, salinity, oxygen, and pressure at 1 dbar intervals

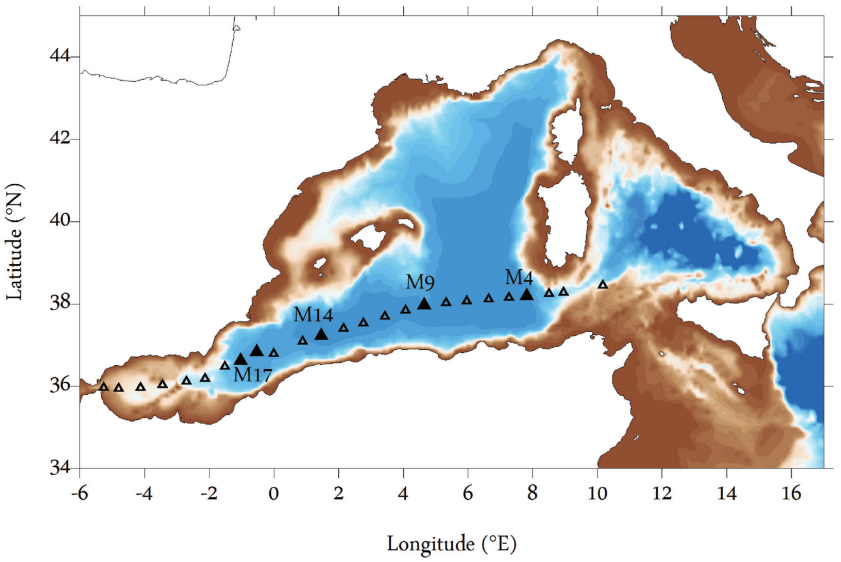

Figure 2. Map of CTD stations that were occupied by R/V *Urania* during 2010. Stations 4 to 17 are part of regular surveys of the western Mediterranean Sea made since 2004 with support from Consiglio Nazionale delle Ricerche (CNR). Here we focus on stations 4 to 17 that were taken during 2006, 2008, and 2010.

exhibit a series of steps and layers through the halocline-thermocline from 600 to 1,400 dbar in most, but not all stations. There were strong steps observed in 2006 at stations 5 to 11, in 2008 at stations 4 to 14, and in 2010 at stations 5 to 9 and 13. Potential temperature, salinity, and density profiles for stations 11 to 17 in 2008 illustrate the stratification through the halocline-thermocline including the strong step and layer structure at stations 11 to 14, which appears to be spatially coherent (Fig. 3). For the eastern stations 4 to 10, the vertical step and layer structures in potential temperature and salinity are jumbled, with no readily apparent pattern even though all stations exhibit strong steps and layers (Fig. 4). In density, however, the similarity of all stations becomes evident. All stations 4 to 10 exhibit layers with the same potential density separated by interfaces with sharp gradients (Fig. 4c). There are generally eight layers at each station. The layers occupy different depth intervals but every station has a layer at each of the eight potential densities. Indeed the more western stations 11 to 17 also exhibit layers at these same densities. These layers have different potential temperatures and salinities but the same densities. We were surprised by the quantum state of the density structure: there are no layers of intermediate density and density increases downward at each station in steps of the same density difference. The overall downward increase in density occurs in eight steps with the density difference between layers appearing to be proportional to the overall background density difference, i.e., larger density difference at 600 to 800 dbar where the background vertical density gradient is larger, and smaller

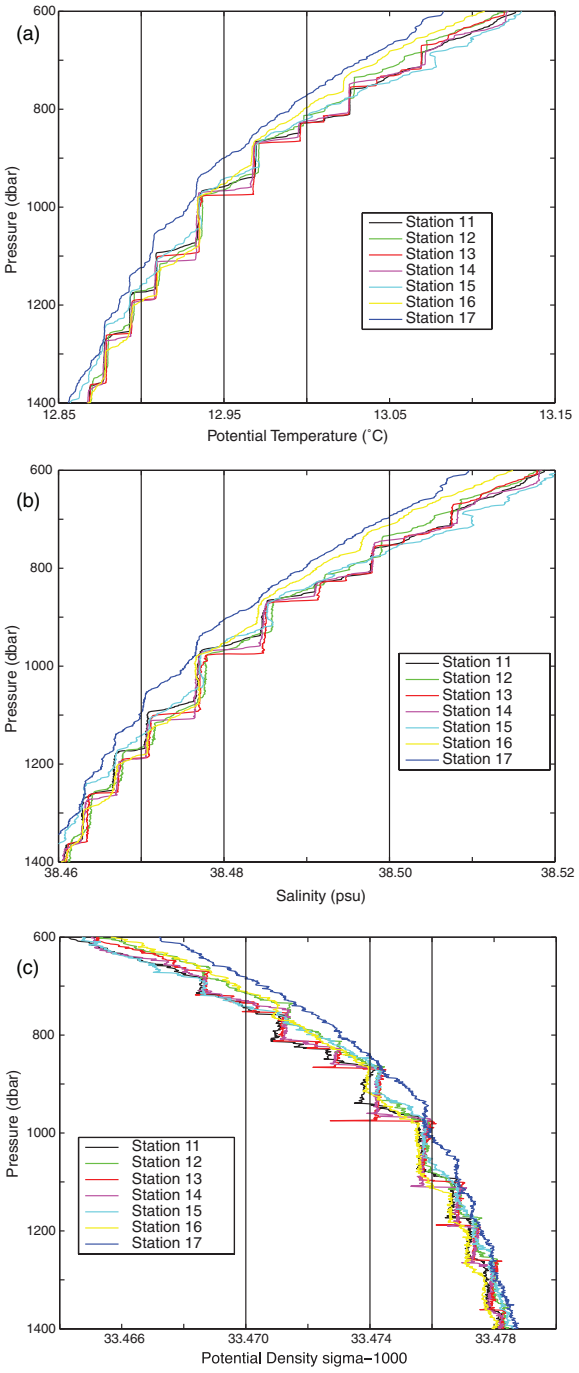

Figure 3. Thermohaline staircase structures in the halocline-thermocline (600 to 1,400 dbar) of the southern western Mediterranean Sea in 2008. Vertical profiles of (a) potential temperature, (b) salinity, and (c) potential density referenced to 1,000 dbar for stations 11 to 17 in Figure 2. Vertical lines are added to enable one to see the slight gradients in the well-mixed layers.

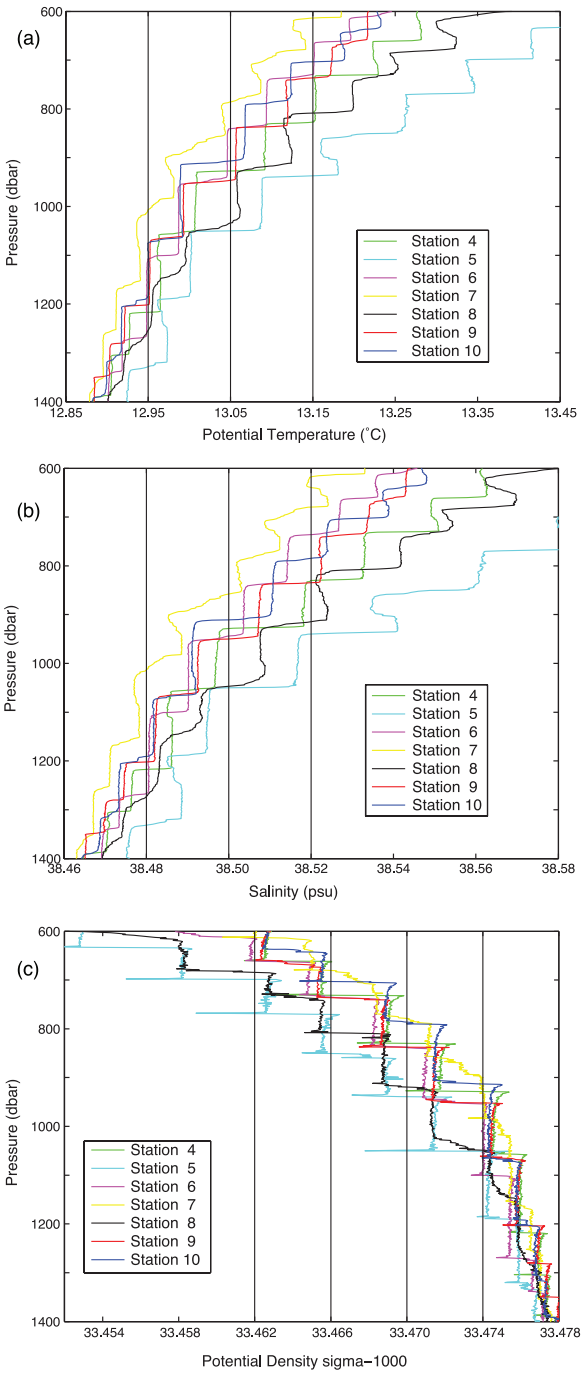

Figure 4. Thermohaline staircase structures in the halocline-thermocline (600 to 1400 dbar) of the southern western Mediterranean Sea in 2008. Vertical profiles of (a) potential temperature, (b) salinity, and (c) potential density referenced to 1000 dbar for stations 4 to 10 in Figure 2. Vertical lines are added to enable one to discern small gradients in the well-mixed layers.

at 1,200 to 1,400 dbar where the background density difference is smaller. Overall for the layers, there is a tendency for potential density (sigma-1000) to decrease very slightly downward through the layers of nearly constant density (Figs. 3c and 4c). Vertical lines of constant density have been added so that the slight slope (where the density in the layers decreases downward) becomes evident. Similarly, there is a tendency for a slight decrease in potential temperature and in salinity downward through the layers. These decreases in temperature, salinity, and density within the layers can be seen in the slopes of layer properties (Fig. 3 and Fig. 4). If we take the relatively continuous profiles of station 16 (shown in yellow in Fig. 3) to represent the background stratification in the region, then the layers are warmer and saltier than the background and the layer density is close to the density at the top of the layer. Thus, the layer structure appears consistent with inputs of temperature, salinity, and density at the top of the layer that are then being convectively mixed downward through the nearly uniform layers.

In terms of water mass characteristics, the layers of same density have different potential temperature—salinity (Theta-S) values at each station; there is a cluster of tight Theta-S values at each station separated from the cluster of Theta-S values at the next station. The spatial pattern is peculiar: for the western stations, highest Theta-S values are at station 5, with progressively lower values at stations 4, 8, 10, 9, 6, and lowest at station 7. This irregular pattern creates confusion whether there are any locations whatsoever where there are intermediate clusters of Theta-S values. On each density surface down to 1,400 dbar, the station order of Theta-S values is the same. Thus, the layers appear to have organized themselves into thick layers of the same density but of different Theta-S characteristics. At each station in the step transition from one density to the next density, the differences in potential temperature and difference in salinity are very large, much greater than the small changes in potential temperature and salinity that would be required to reach the next density. The step changes in Theta and S are thus nearly parallel to the density surface with only a small cross-isopycnal component.

Over time from 2006 to 2008 to 2010, we could not identify consistent evolution of step and layer structure over time. Only stations 5 to 9 had strong steps and layers in all three years and the time varying structure for station 9 illustrates the difficulty in identifying consistent layers (Fig. 5). Since the layers are moving about with the currents, we should not expect to see consistent temporal evolution of properties at a fixed site.

As is clear in the density profiles (Fig. 3c and 4c), there are typically eight steps between 600 and 1,400 dbar separating layers where the potential temperature, salinity, and potential density are uniform. For example, vertical differencing potential temperature over one dbar between 600 and 1,400 dbar for station 10 in 2008 (Fig. 6) shows that 540 out of 800 differences are within 0.0001 °C; the seven complete layers between 600 and 1,400 dbar have thicknesses of 57, 70, 110, 149, 117, 98, and 69 dbar (as defined by vertical differences less than 0.0015 °C) for an average thickness of 96 dbar (Table 1). The eight steps defined by the intervals between these layers have thicknesses varying from 5 to 16 dbar with an average of 11 dbar. The largest step occurs at 705 dbar where the temperature and salinity

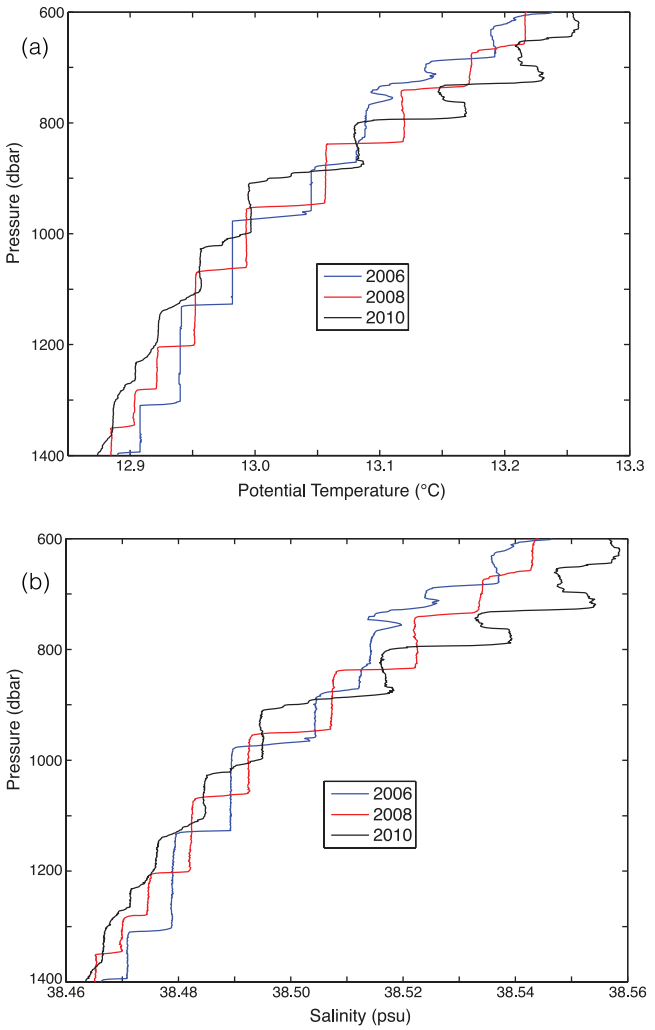

Figure 5. Staircase structure at station 9 in 2006, 2008, and 2010: (a) potential temperature and (b) salinity.

change by 0.061 °C and 0.012 respectively. For stations 4 to 13 with the most pronounced steps and layers, the layers have an average thickness of 93 dbar and the eight steps have an average thickness of 7 dbar. Thus, the staircase structure changes the large-scale background vertical structure of salinity, potential temperature, and density profiles from 600 to 1,400 dbar into a series of eight layers averaging 93 dbar in thickness separated by steps of sharp gradients averaging seven dbar in thickness. The vertical changes in these steps are much larger than the background gradients and they account for 95% of the changes in temperature and salinity from 600 to 1,400 dbar.

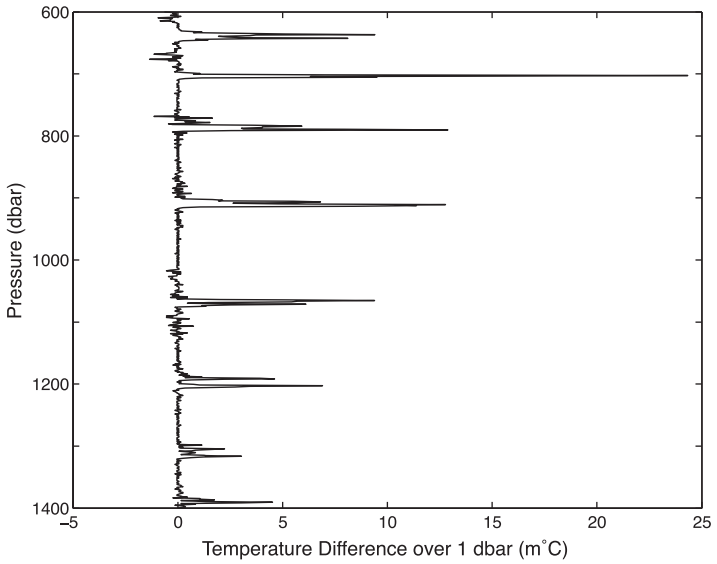

Figure 6. Vertical difference in potential temperature through the staircase structures at station 10. Vertical differences taken over 1 dbar are shown in millidegrees. The layers are clearly identified by near-zero differences, separated by sharp spikes of large differences indicative of the steps.

Table 1. Layers properties for station 10. Potential temperature (Theta), salinity, and potential density relative to 1,000 dbar (Sigma1). Only complete layers between 600 and 1,400 dbar are considered. The differences in potential temperature (deltaTh) and in salinity (deltaS) are estimated by taking the difference between Theta and salinity in the layer above minus Theta and salinity in the layer below. $R_\rho = \alpha^*\text{deltaTh}/(\beta^*\text{deltaS})$ where α and β are the thermal expansion and haline contraction coefficients respectively, is estimated using α and β calculated for each layer's pressure, temperature, and salinity.

Pressure		Theta	Salinity	Sigma1	deltaTh	deltaS	R_ρ
644	701	13.186	38.538	33.4656	.1065	.0238	1.29
706	776	13.123	38.524	33.4691	.1193	.0274	1.26
792	902	13.067	38.511	33.4717	.1319	.0322	1.19
914	1063	12.991	38.492	33.4746	.1170	.0292	1.18
1073	1190	12.950	38.482	33.4758	.0744	.0187	1.18
1206	1304	12.917	38.473	33.4769	.0508	.0131	1.16
1317	1386	12.899	38.468	33.4773	.0325	.0088	1.11

3. Estimating vertical fluxes associated with salt finger staircases

In 2005 and 2006 there were major deep water formation events in the northwestern Mediterranean (Schroeder et al., 2006; Schroeder et al., 2008: Smith et al., 2008; Grignon et al., 2010, Schroeder et al., 2010). Deep convection occurred over a large area of the

northwestern Mediterranean in marked contrast to the localized deep water formation in the Gulf of Lion that has been traditionally observed (MEDOC Group, 1970). A large volume of new dense water was formed which subsequently spread out from its formation region and filled the western Mediterranean below about 2,300 m. Remarkably, the new deep water was warmer, saltier and denser than the old deep water. After the 2006 convection, the water column stratification consists of the halocline-thermocline from 400 to 1,500 m depth, some old deep water at the base of the halocline-thermocline, and then a transition region from the bottom of the old colder, fresher deep water to the new warmer, saltier deep water (Fig. 7). This transition region becomes progressively warmer and saltier from 2006 to 2008 to 2010 at all stations 4 to 17 suggesting a convergence of heat and salt into the transition region. In terms of vertical mixing processes, the observed convergence of heat and salt could be due either to downward fluxes of heat and salt through the halocline-thermocline associated with salt finger processes or to upward fluxes of heat and salt from the new deep water associated with diffusive convection in the transition between old and new deep waters where temperature is stabilizing while salinity is destabilizing. Because diffusive convection is generally less effective than salt finger mixing (Turner, 1967), we attribute the convergence of heat and salt to salt finger processes transporting heat and salt downward through the halocline thermocline.

We estimate the convergence of heat and salt in this transition zone by calculating the increase in temperature and salinity over time in this zone from 2006 to 2008 (Table 2) and from 2008 to 2010 (Table 2). For each station we examine the 2006 and 2008 potential temperature and salinity profiles (Fig. 7 shows sample profiles from Station 10) and identify the upper pressure surface where the properties are the same in both 2006 and 2008 and the lower pressure surface where the properties are the same in both years. The upper surface is effectively the bottom of the halocline-thermocline and the lower surface is the top of the new deep water. We examine the 2006 to 2008 differences in potential temperature and salinity in this convergence zone, note the maximum differences, and calculate the depth integrated differences labeled Sbulk and ThBulk (Table 2). For all stations, the 2006 to 2008 differences are positive, that is warmer and saltier in 2008, indicating that heat and salt have been added to the transition region between the bottom of the halocline-thermocline and the top of the new deep water. We do a similar procedure for the 2008 and 2010 potential temperature and salinity profiles (Table 2) and again for all stations the 2008 to 2010 differences are positive representing warmer and saltier values in 2010.

There are inherent uncertainties in salinity of order 0.002 and temperature of 0.001 °C between surveys that lead to uncertainties in Sbulk and Thbulk of order 1 psu m and 0.5 °C m. The maximum differences are clearly above these uncertainties and nearly all of the bulk differences exceed their uncertainty thresholds. Thus, there is clear warming and salinification from 2006 to 2008 to 2010 in the depth interval between the bottom of the halocline-thermocline and the top of new deep water.

From examination of the profiles, it appears that for many of the 2006 stations new deep waters are still arriving: the thickness of the deep water is only 200 m or so compared to the

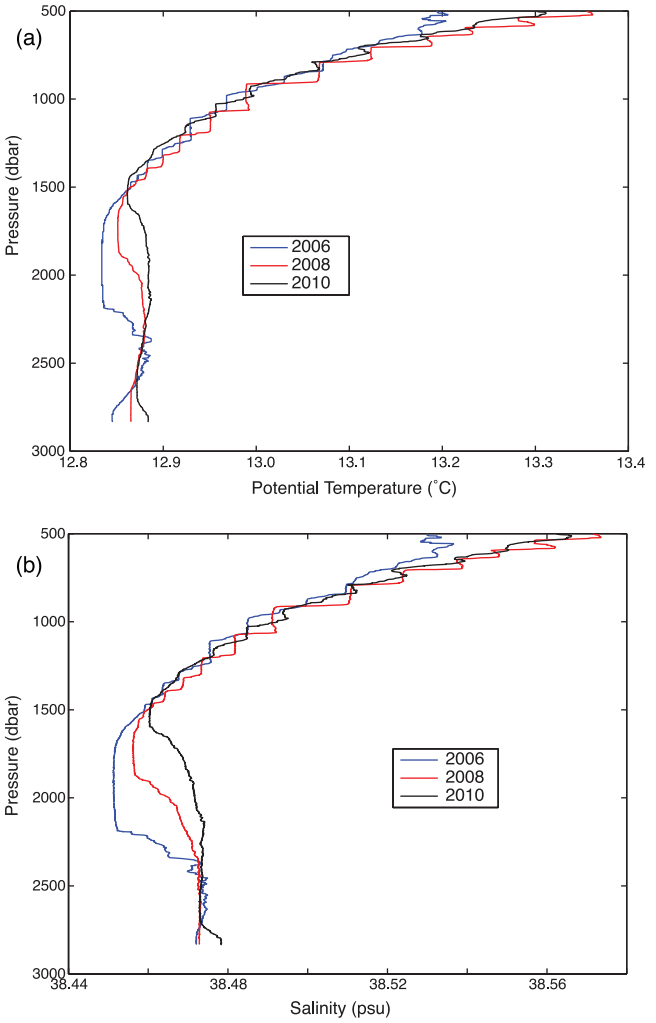

Figure 7. Profiles of (a) salinity and (b) potential temperature below 500 dbar at station 10 for 2006, 2008, and 2010 surveys. The halocline-thermocline from 400 dbar to 1,500 dbar exhibits step-like features that are associated with salt finger processes; the deep waters below 2,300 dbar exhibit similar characteristics of new deep water formed in 2005 to 2006. The only part of the water column where changes are immediately evident is the transition zone between the bottom of the halocline-thermocline and the top of the new deep water. Here the transition waters become progressively warmer and saltier from 2006 to 2008 to 2010. The differences between the 2008 and 2006 profiles and the differences between the 2010 profiles and the 2008 profiles in the transition zone between the bottom of the halocline-thermocline and the top of the new deep water are used to quantify the amount of salt and heat flux convergences into this transition zone, tabulated in Table 2.

Table 2. Differences in salinity and potential temperature from 2006 to 2008 and from 2008 to 2010 for stations across the southern western Mediterranean Sea. The pressure interval over which differences are estimated are given by top and bottom pressures. The maximum differences over this interval are significant above the uncertainties in salinity of 0.002 and in temperature of 0.001°C. The bulk differences are vertical integrals of the differences over the pressure interval for each station. For these bulk values, we find it useful to use the psu symbol for salinity so the units of the vertical integral are clear. The ratios are intended to provide an indication of whether these changes represent increases or decreases in density: for ratios less than 3.1 = β/α (= haline contraction coefficient divided by thermal expansion coefficient) these salinity and temperature increases represent increases in density. Because the new deep waters formed in 2005 to 2006 do not appear to have completed their penetration to these southern sites by the time of the 2006 survey, we argue that the salinity and potential temperature changes from 2008 to 2010 are more representative of downward fluxes associated with salt finger processes.

Station	Top (dbar)	Bottom (dbar)	ΔSmax	Ratio ΔTh/ΔS	ΔThmax °C	Sbulk psu m	Ratio Th/S	ThBulk °C m
2006–2008								
4	1570	2440	0.015	2.6	0.040	6.81	2.5	16.99
5	1910	2365	0.018	2.4	0.044	5.43	2.5	13.81
7	1665	2395	0.019	2.5	0.048	8.60	2.5	21.88
9	1660	2310	0.018	2.5	0.044	6.40	2.6	16.85
10	1520	2350	0.017	2.5	0.044	6.88	2.7	18.50
11	1605	2540	0.017	2.6	0.045	9.98	2.5	25.29
12	1500	2530	0.018	2.7	0.047	9.25	2.7	24.77
13	1595	2270	0.009	2.7	0.024	3.78	2.7	10.16
14	1570	2600	0.012	2.6	0.031	6.20	2.8	14.49
15	1640	2540	0.023	2.5	0.057	13.97	2.4	33.73
16	1625	2470	0.016	2.5	0.041	8.62	2.4	20.87
17	1590	2450	0.020	2.3	0.048	12.01	2.3	27.55
Average				2.5		8.24	2.5	20.66
2008–2010								
4	1570	2070	0.012	2.3	0.026	3.50	2.1	7.46
5	1670	2125	0.010	2.2	0.022	2.46	2.1	5.09
6	1600	2130	0.011	2.3	0.027	2.87	2.2	6.23
7	1540	2100	0.010	2.4	0.023	2.39	2.0	4.80
8	1785	1920	0.006	1.9	0.012	0.55	1.7	0.96
9	1520	2300	0.014	2.5	0.039	5.65	2.3	12.78
10	1500	2250	0.014	2.3	0.032	5.56	2.1	11.57
11	1600	2300	0.009	2.8	0.025	3.04	2.6	7.92
12	1550	2260	0.006	2.5	0.014	2.07	2.4	4.95
13	1500	2230	0.004	2.7	0.010	0.97	2.9	2.79
14	1450	2200	0.012	2.6	0.030	4.18	2.5	10.30
15	1750	2350	0.006	2.5	0.014	1.04	2.0	2.07
16	1500	2100	0.011	2.7	0.029	4.21	2.7	11.45
17	1450	2050		2.5	0.024	3.10	2.5	7.73
Average				2.4		2.97	2.3	6.86

600 m thickness in 2008 and 2010 and the gradients from the old deep water to the new deep water are very sharp indicating new deep water is still intruding at depth. Stations 9 (Bryden et al., 2014, Fig. 3) and 10 (Fig. 7) appear to be the only locations where the new deep water has fully arrived in 2006. For this reason, we are not confident that the increased temperature and salinity in the transition region from 2006 to 2008 represents just salt finger fluxes since arrival of new deep water would also increase the temperature, salinity, and thickness of the deep water from 2006 to 2008. Hence, we focus on the increases of temperature and salinity from 2008 to 2010, where the properties of the new deep water appear to be stable from 2008 to 2010, for quantitative estimates of salt finger fluxes (Table 2).

The vertically integrated salinity and potential temperature increases over the transition zone from November 2008 to August 2010 amounted to 3.0 psu m and 6.9 °C m when averaged over stations 4 to 17 (Table 2). Dividing these salinity and temperature increases by the 640 days between the 2008 and 2010 surveys, we estimate a salt flux convergence of 5.35×10^{-8} psu m s^{-1} and a heat flux convergence of 12.4×10^{-8} °C m s^{-1}. Multiplying these convergences by gravity, haline contraction (α), and thermal expansion (α) coefficients respectively (evaluated at $S = 38.475$, $\theta = 12.88$ °C and $p = 2000$ dbar) yields buoyancy flux convergences of $g\beta F_S = 3.97 \times 10^{-10}$ W kg^{-1} (due to salinity convergence) and $g\alpha F_T = 2.94 \times 10^{-10}$ W kg^{-1} (due to heat convergence) for a net density flux convergence of 1.0×10^{-10} W kg^{-1}. The buoyancy flux ratio, $\alpha F_T/\beta F_S$, is then 0.74.

4. Modeling salt and heat fluxes associated with salt finger processes

Dividing downward fluxes of salt and heat, $F_S = 5.35 \times 10^{-8}$ psu m s^{-1} and $F_T = 12.4 \times 10^{-8}$ °C m s^{-1} by the average vertical gradients of salinity and temperature, $dS/dz = 0.953 \times 10^{-4}$ psu m^{-1} and $d\Theta/dz = 4.09 \times 10^{-4}$ °C m^{-1}:

$$F_S = k_S dS/dz \quad \text{and} \quad F_T = k_T d\Theta/dz$$

provides estimates of bulk salinity and temperature mixing coefficients, $k_S = 5.6 \times 10^{-4}$ m^2 s^{-1} and $k_T = 3.0 \times 10^{-4}$ m^2 s^{-1}. Such bulk mixing coefficients are typical of those identified in laboratory experiments (Turner, 1967) and in the western tropical Atlantic beneath the Subtropical Underwater tongue (Lambert and Sturges, 1977). From tracer dispersion and microstructure observations in the tropical Atlantic thermocline, Schmitt et al. (2005) estimated $k_S = 0.9 \times 10^{-4}$ m^2 s^{-1} and $k_T = 0.45 \times 10^{-4}$ m^2 s^{-1}, a factor of five smaller than our bulk mixing coefficients for the Mediterranean. In each case the salinity coefficient is about twice as large as the temperature coefficient, which is typical for salt finger processes that are more efficient at mixing salt than heat. The Mediterranean bulk mixing coefficients are larger than traditional values of basin-scale diffusivities of order 1×10^{-4} m^2 s^{-1} (Munk, 1966) and that is again a feature of salt finger processes that are thought to be more efficient at mixing salt and heat vertically than are mechanical mixing processes associated with eddies and internal waves.

Such bulk mixing coefficients are deceptive, however, in the sense that mixing within the uniform layers of constant salinity, potential temperature, and density is virtually infinite and the only substantial vertical gradients are in the interfaces or steps where salt finger processes are operating and there the vertical gradients are much larger than the background gradients. Typical laboratory and theoretical analyses attempt to define the mixing coefficients operating on these sharper gradients. To define such salt finger mixing coefficients, we use the observed step structures to argue that the overall vertical salinity and potential temperature gradients between 600 and 1,400 dbar are actually done in eight steps with thickness averaging 7 dbar. Thus, the gradients in the halocline-thermocline are not due to smooth change from 600 to 1,400 dbar but rather are due to eight discrete steps, so that the effective vertical gradients occur over a total of 56 m rather than 800 m. Hence the effective vertical gradients in the steps are 15 times larger than the background gradients and we would estimate the mixing coefficients associated with salt finger processes operating in these steps to be 15 times smaller than the bulk coefficients: typical k_S and k_T for the steps are then $k_S = 3.7 \times 10^{-5}$ m^2 s^{-1} and $k_T = 2.0 \times 10^{-5}$ m^2 s^{-1} to achieve the salt and heat transports across the steps.

In developing a theory for salt finger mixing, Kunze (1987) argued that the size of the mixing coefficient associated with salt finger processes acting over a sharp vertical transition in salinity and temperature between layers is proportional to the molecular viscosity ν, $(= 1 \times 10^{-6}$ m^2 s$^{-1})$, rather than the molecular diffusion coefficients for salt and heat (of order 10^{-9} and 10^{-7} m^2 s^{-1}). He found that the maximum fluxes should be inversely proportional to Ri (Richardson number taken equal to 1/4), and proportional to a complicated function of the flux ratio:

$$\text{Maximum Salt Flux} = F_S = (0.5/Ri)^* \nu^* (sqrt(R_\rho) + sqrt(R_\rho - 1))^{2*} dS/dz.$$

With this formulation and a density ratio of 1.28, we would estimate the theoretical salt mixing coefficient within the layers to equal $k_S = (0.5/Ri)^* \nu^* (sqrt(R_\rho) + sqrt(R_\rho - 1))^2 = 2.2 \times 10^{-5}$ m^2 s^{-1}, within a factor of two of our estimate above based on the gradients in seven steps of average thickness six meters. Kunze (1987) went further, however, and argued that the average fluxes should be this maximum flux divided by a constant, σ_t, defined by the time scale for a small perturbation to grow to maximum finger length. σ_t is dependent on the density ratio and defined by Kunze's (1987) equation 19 and we estimate σ_t to be 3.5 for a flux ratio of 1.28. Thus, we estimate Kunze's theoretical salt finger mixing formulation to yield an average salt finger mixing coefficient:

$$k_S = \text{Maximum Salt Flux}/(dS/dz^* \sigma_t) = (0.5/Ri)^* \nu^* (sqrt(R_\rho) + sqrt(R_\rho - 1))^2/\sigma_t$$

equal to 1.6×10^{-6} m^2 s^{-1} which is an order of magnitude smaller than our estimate above of 3.7×10^{-5} m^2 s^{-1}. In Kunze's (1987) theoretical formulation, the interfaces are very thin, of order 0.5 m, so the vertical gradients are much larger than we find for the steps with thickness of order seven meters and the accompanying theoretical mixing coefficient can

be very small. It may well be the case that the CTD cannot resolve the very thin steps of 0.5 m, but we have examined the CTD measurements across the steps (the transitions between layers of constant properties) and we remain convinced that the property gradients do actually occur over vertical scales of at least a few meters. Thus, the fundamental difference between observations and Kunze's (1987) model of salt finger step structure is that the observations indicate thicker steps of several meters while the model assumes thin steps of order 0.5 m with very large gradients over which relatively small diffusivities can affect the vertical salt and heat transports.

Radko and Smith (2012) have recently put forward a model where the linear growth of salt fingers to finite amplitude is balanced by secondary instabilities in the salt fingers. The layer of active salt finger mixing is thicker than the salt finger scale of maximum growth rate (about 0.5 m), in agreement with our observations for an order 7 m thickness for the sharp gradients steps, though they did not explicitly give the vertical scale of the salt finger zone. Radko and Smith (2012) made predictions for the heat and salt fluxes (and buoyancy flux ratio) as a function of R_ρ. For the observed background stratification in our observations of the western Mediterranean, R_ρ equals 1.28, for which their model produces mixing coefficients of $k_S = 3.5 \times 10^{-5}$ m^2 s^{-1} and $k_T = 1.7 \times 10^{-5}$ m^2 s^{-1}, and a buoyancy flux ratio of 0.62. Their mixing coefficients are similar to those we estimate above for the eight sharp gradient regions (3.7 and 2.0×10^{-5} m^2 s^{-1}) where we divided the bulk mixing coefficients by a factor of 15 to reflect the mixing in the sharp gradient regions where salt finger processes are active. Their predicted buoyancy flux ratio is slightly lower than our observed value of 0.72. Their theory is dependent on choosing an adjustable coefficient that is then calibrated with numerical simulations; and our observational estimates could easily be off by a factor of two. Nevertheless, the agreement is notable, certainly superior to the fluxes based on traditional salt finger theory for very thin interfaces.

Radko's (2005) theory also predicts the equilibrium height of layers as a function of R_ρ, again after choosing one adjustable coefficient. For the Mediterranean observations described here where R_ρ equals about 1.1 to 1.3, Radko (2005) estimated layer thicknesses greater than 200 m for his adjustable coefficient $C_L/C = 1000$. Our observed layer thicknesses are of order 100 m, they do appear to increase from 50 m to 150 m for decreasing R_ρ values from 1.3 to 1.18 (Table 1) in agreement with the model, but then the thicknesses decrease as R_ρ decreases to 1.11 contrary to the theory. Quantitatively, there is a general agreement of the observed and modeled layer thicknesses when the adjustable coefficient C_L/C is chosen to be 500 instead of 1,000. This is a case where the observations can help to guide the choice of a single adjustable model parameter. In the lower parts of the halocline-thermocline where R_ρ approaches 1.1, the thickness of the layers may be limited by their closeness to the bottom boundary of the halocline-thermocline representing the transition into the more homogeneous deep water layer. This bottom boundary appears to shallow from 1,600 to 1,500 to 1,400 m depth from 2006 to 2008 to 2010 (Fig. 7). Our interpretation of Radko's theory is that it is an interior solution for a halocline-thermocline away from boundaries. Certainly the lowest layer from 1,317 to 1,386 dbar (Table 1) is close to the

bottom of the halocline-thermocline. Observations of "interior" layers in regions with lower and higher R_ρ values may help development of the theory for the equilibrium thickness of layers.

5. Discussion

The downward temperature and salinity fluxes associated here with the salt finger mixing processes in the halocline-thermocline are sufficient to warm a 1,000 m layer in the deep water by 0.019°C and to salinify a 1,000 m layer by 0.0017 over one year. Such warming and salting should be persistent over time as long as the halocline-thermocline below the LIW persists. Borghini et al. (2014) have documented warming and salting in the deep western Mediterranean of this magnitude over the past 40 years. The downward density flux associated with salt finger mixing and calculated here from the sum of the heat and salt fluxes multiplied by thermal expansion and haline contraction coefficients is quite small, only 0.00032 kg m^{-3} for a 1,000 m thick deep water layer over a year, equivalent to only 0.013 kg m^{-3} over 40 years. It is not clear whether the western Mediterranean deep waters have increased their density over 40 years by even 0.01 kg m^{-3} because such accuracy is a challenge for historical observations.

It is rare to have observational estimates of the downward fluxes of salt and heat associated with salt finger processes. Normally, heat (and salt) fluxes are estimated from microstructure profiles linking the mechanical energy dissipation in the profiles to potential energy generation by salt finger processes (e.g., St. Laurent and Schmitt, 1999). We could only find a single estimate of salt finger fluxes based on observed convergences of heat and salt by Hebert (1988) beneath a Mediterranean eddy, and this analysis suffered from uncertainty in the definition of the boundaries of the convergence zone over time. Here we are able to compare the vertical fluxes of salt and heat down through the halocline-thermocline in the western Mediterranean, as quantified by time changes in salinity and temperature at the base of the halocline-thermocline from repeat surveys two years apart, with the observed properties of thermohaline staircase structures that define both the background stratification and the vertical gradients within the steps and layers. The mixing coefficients based on the salt and heat fluxes acting on the background stratification are large, of order 3 to 6×10^{-4} m^2 s^{-1}. Mixing coefficients based on the vertical gradients in the steps are of order 2 to 4×10^{-5} m^2 s^{-1}, still an order of magnitude greater than those traditional theory for salt finger growth would suggest (eg. Kunze, 1987), but in apparent agreement with recent model results where salt finger growth is arrested by secondary instabilities (Radko and Smith, 2012).

Previous estimates of salt finger fluxes in the open ocean derived from microstructure measurements that link turbulent mechanical energy dissipation (measured) with potential energy generation by salt finger processes (inferred) are made uncertain by the amount of background mechanical mixing present in the ocean associated with internal waves and shear dissipation. In the quiet Mediterranean with relatively weak circulation, low winds and

small tides, the amount of background mechanical mixing may be less of an issue, so in the Mediterranean the amount of turbulent mechanical energy dissipation may be more closely aligned with the potential energy generation by salt finger processes, especially in the deep halocline-thermocline where thermohaline staircases are observed. We encourage attempts to use microstructure profilers to measure the amount of mechanical and thermodynamic mixing in Mediterranean thermohaline staircases, both in the sharp steps of order 4 to 10 m and in the thick nearly homogeneous layers with order 95 m thickness to assess whether the fluxes of heat and salt and the associated downward density flux estimated here are of a size to match the turbulent dissipation in the steps and layers.

Observing heat and salt flux convergences over time can offer an accurate method for determining the fluxes of heat and salt in salt finger regimes. Relatively simple observations of convergences from repeat surveys in different salt finger regimes could offer a way to quantify the size of salt finger fluxes under different environmental conditions and thereby lead to accurate parameterization for the effects of salt fingers in circulation models. Furthermore, both observed fluxes and turbulent mixing profiles could be compared with theoretical and laboratory-based models of salt finger fluxes and associated thermohaline staircase structures to assess the reliability of the models in representing open ocean salt finger mixing processes.

Acknowledgments. We thank CNR for continuing support for sustained observations in the Mediterranean Sea. The Captain and Officers of R/V Urania ensured the safe and efficient scientific operations on all expeditions. HLB thanks the Leverhulme Trust for supporting his involvement in this Mediterranean research. We thank CNR-IAMC (Oristano-Italy, and in particular Dr. Alberto Ribotti) for providing additional profiles that were used for comparison and quality control. Timour Radko and Raymond Schmitt provided enthusiastic, critical reviews that led to improved comparisons with previous observations and theory.

REFERENCES

Borghini, M., H. Bryden, K. Schroeder, S. Sparnocchia and A. Vetrano. 2014. The Mediterranean is getting saltier. Ocean Sci. Discuss., *11*, 735–752, doi:10.5194/osd-11-735-2014.

Bryden, H., K. Schroeder, M. Borghini, A. Vetrano and S. Sparnocchia. 2014. Mixing in the deep waters of the western Mediterranean, in The Mediterranean Sea: Temporal Variability and Spatial Patterns, Geophysical Monograph 102, edited by G. E. Borzelli, M. Gacic, P. Lionello and P. Malanotte-Rizzoli, pp. 51–58, American Geophysical Union and John Wiley & Sons.

Grignon, L., D. A. Smeed, H. L. Bryden and K. Schroeder. 2010. Importance of the variability of hydrographic preconditioning for deep convection in the Gulf of Lion, NW Mediterranean, Ocean Sci., *6*, 573–586.

Hebert, D. 1988. Estimates of salt finger fluxes, Deep Sea Res. A, *35*, 12, 1887–1901, doi:10.1016/0198-0149(88)90115-X.

Johannessen, O. M. and O. S. Lee. 1974. A deep stepped thermo-haline structure in the Mediterranean, Deep Sea Res. A, *21*, 8, 629–639, doi:10.1016/0011-7471(74)90047-3.

Katz, E. J. 1972. The Levantine Intermediate Water between the Strait of Sicily and the Strait of Gibraltar, Deep Sea Res. A, *19*, 7, 507–520, doi:10.1016/0011-7471(72)90018-6.

Kunze, E. 1987. Limits on growing, finite-length salt fingers: A Richardson number constraint, J. Mar. Res., *45*, 3, 533–556, doi:10.1357/002224087788326885.

Lambert, R. B., Jr. and W. Sturges. 1977. A thermohaline staircase and vertical mixing in the thermocline, Deep Sea Res. A, *24*, 3, 211–222, doi:10.1016/S0146-6291(77)80001-5.

MEDOC Group. 1970. Observation of formation of deep water in the Mediterranean Sea, 1969, Nature, *227*, 1037–1040.

Molcard, R. and R. I. Tait (1977) The steady state of the step structure in the Tyrrhenian Sea, in A Voyage of Discovery, edited by M. V. Angel. pp. 221–233. Pergamon Press.

Munk, W. H. 1966. Abyssal recipes, Deep Sea Res. A, *13*, 4, 707–730, doi:10.1016/0011-7471(66)90602-4.

Radko, T. 2005. What determines the thickness of layers in a thermohaline staircase? J. Fluid Mech., *523*, 79–98, doi:10.1017/S0022112004002290.

Radko, T. and D. P. Smith. 2012. Equilibrium transport in double-diffusive convection, J. Fluid Mech., *692*, 5–27, doi:10.1017/jfm.2011.343.

St. Laurent, L. and R. W. Schmitt. 1999. The contribution of salt fingers to vertical mixing in the North Atlantic Tracer Release Experiment, J. Phys. Oceanogr., *29*, 7, 1404–1424, doi:10.1175/1520-0485(1999)029.

Schmitt, R. W., J. R. Ledwell, E. T. Montgomery, K. L. Polzin and J. M. Toole. 2005. Enhanced diapycnal mixing by salt fingers in the thermocline of the tropical Atlantic, *Science, 308*, 5722, 685–688, doi:10.1126/science.1108678.

Schroeder, K., G. P. Gasparini, M. Tangherlini and M. Astraldi. 2006. Deep and intermediate water in the western Mediterranean under the influence of the Eastern Mediterranean Transient, Geophys. Res. Lett., *33*, L21607, doi:10.1029/2006GL027121.

Schroeder, K., A. Ribotti, M. Borghini, R. Sorgente, A. Perilli and G. P. Gasparini. 2008. An extensive western Mediterranean deep water renewal between 2004 and 2006, Geophys. Res. Lett., *35*, L18605, doi:10.1029/2008GL035146.

Schroeder K., S. A. Josey, M. Herrmann, L. Grignon, G. P. Gasparini and H. L. Bryden. 2010. Abrupt warming and salting of the Western Mediterranean Deep Water after 2005: Atmospheric forcings and lateral advection, J. Geophys. Res., *115*, C08029, doi:10.1029/2009JC005749.

Smith, R. O., H. L. Bryden and K. Stansfield. 2008. Observations of new western Mediterranean deep water formation using Argo floats 2004–2006, Ocean Sci., *4*, 133–149.

Turner, J. S. 1967. Salt fingers across a density interface, Deep Sea Res. A, *14*, 599–611, doi:10.1016/0011-7471(67)90066-6.

Turner, J. S. 1973. Buoyancy Effects in Fluids, Cambridge University Press, 367 pp.

Zodiatis, G. and G. P. Gasparini. 1996. Thermohaline staircase in the Tyrrhenian Sea, Deep Sea Res., *43*, 5, 655–678, doi:10.1016/0967-0637(96)00032-5.

Received: *1 January 2014*; revised: *27 March 2014*.